IET Generation, Transmission & Distribution

Research Article

IET Journals
The Institution of Engineering and Technology

Optimal energy storage system allocation and operation for improving wind power penetration

ISSN 1751-8687
Received on 30th June 2014
Revised on 5th April 2015
Accepted on 16th July 2015
doi: 10.1049/iet-gtd.2014.1168
www.ietdl.org

Le Zheng ✉, *Wei Hu*, *Qiuyu Lu*, *Yong Min*

State Key Laboratory of Power Systems, Department of Electrical Engineering, Tsinghua University, Beijing 100084, People's Republic of China
✉ *E-mail: zhengl07@mails.tsinghua.edu.cn*

Abstract: In recent years, the energy storage system (ESS) has been demonstrated to be involved in many aspects of the integration of wind power. For ESS application, ESS allocation of the installation location, power rating, and energy rating is the first concern. Different from previous studies, this study emphasises the significance of the ESS operation in the study of ESS allocation. A bi-level-programming-based model is proposed to take the interaction of allocation and operation into consideration at the same time, with the external level optimising allocation and the internal level optimising operation. The complexity assessment and solution algorithm of the model is also discussed. Next, a genetic numerical algorithm is proposed to solve the bi-level model. The authors' results were tested on a modified IEEE 39 bus system and a provincial regional power system to verify both the flexibility and applicability of the proposed model and algorithm. This model is useful for various types of ESS and provides a foundation for ESS application.

Nomenclature

C_{total}	total cost per day
$C_{\text{operation}}$	operation cost per day
$C_{\text{investment}}$	ESS investment cost per day
$C_{\text{generation}}$	generation cost per day
P^{r}_{sk}, E^{r}_{sk}, T_{sk}	the kth ESS power rating, energy rating, and lifetime
η_{Pk}, η_{Ek}, η_{Mk}	the kth ESS power cost per kW, energy cost per kWh, operation and maintenance cost per day
W_{loss}, η_{loss}	total power loss of a specific day and electricity price
g, w, s, L	subscripts that denote fossil-fuel generator, wind farm, ESS, and load, respectively
$P_{xi,t}$, $Q_{xi,t}$	active and reactive power of x of bus i at period t, respectively, x represents one of the subscripts g, w, s, L
$P_{\text{L},t}$, $Q_{\text{L},t}$	system active and reactive load at period t
G_{ij}, B_{ij}	real part and imaginary part of bus admittance matrix at ith row and jth column
$\theta_{ij,t}$	voltage angle difference between buses i and j at period t
$V_{i,t}$, $V_i^{\min}$, $V_i^{\max}$	voltage magnitude at period t and range of bus i
$P_{\text{s}}^{\min}$, $P_{\text{s}}^{\max}$, $E_{\text{s}}^{\min}$, $E_{\text{s}}^{\max}$	ESS power and energy rating range, determined by investors
$P_{lij,t}$, $P_{lij}^{\max}$	power magnitude at period t and limit through line ij
a_i, b_i, c_i	cost coefficients of fossil-fuel generator i
N_x, N	number of x and buses in the system, x represents one of the subscripts g, w, s, L
T, Δt	number of time intervals (24 h) and duration of each period
η_{w}	wind curtailment fee
R_t	spinning reserve at period t
$P_{\text{w}j}^{\text{pre}}$	active power limit of the jth wind farms according to prediction
$P_{gi}^{\min}$, $P_{gi}^{\max}$	active power range of the ith fossil-fuel generators
r_{gi}	ramp rate of generator i
$E_{sk,t+1}$, $E_{sk,t}$	energy stored in the kth ESS at period $t+1$ and t, respectively
λ_{sk}	efficiency of ESS charging/discharging

1 Introduction

Due to the growing awareness of the limited supply of fossil fuels and environmental concerns, an interest in renewable energy, particularly in wind energy, has grown significantly in recent years. By 2013, the total capacity of wind power generation in China (excluding Taiwan) has reached 91,412 MW with a growth rate of 21.4% [1]. Unlike European or American patterns, large-scale grid-connected wind power has a high priority in China. However, high wind power penetration addresses numerous problems, such as power fluctuation and voltage stability [2]. Incorporating the energy storage system (ESS) with wind farms is a novel idea that is being actively researched [3–12]. The incorporation of ESS into applications, such as generation scheduling and unit commitment is critical for improving system performance and decreasing wind curtailment.

Several approaches for allocating or operating ESS have been developed. In [3], the optimal allocation, including installation location, sizing, and scheduling of ESS, was developed in distribution systems, whereas Mohammadi *et al.* [4] provided a stochastic scenario-based model to estimate the profit of the ESS projects to determine the size of ESS application in micro-grid. Ross *et al.* [5], Yuan *et al.* [6], and Daneshi and Srivastava [7] focused on obtaining optimal generation scheduling, which included hourly output power of ESS, to minimise the production cost of the entire system. From another perspective, Brekken *et al.* [8] proposed several different control strategies, with an emphasis on comparing which strategy can maximise the system with minimal cost.

Atwa and El-Saadany [3], Mohammadi *et al*. [4], Ross *et al*. [5], Yuan et al. [6], Daneshi and Srivastava [7], Brekken *et al*. [8], and Teleke *et al*. [9] considered the ESS allocation and operation separately, but ESS allocation could have a great effect on the operation. For example, different ESS installation locations resulted in different power flows, such as to affect the power loss of the entire power grid, particularly when the power system faced congestion problems. In addition, the sizing and scheduling of the ESS affected the generation scheduling of the conventional generators. Thus, it is important to combine the allocation and operation together. Chen and Duan [10], Zheng *et al*. [11], and Chakraborty *et al*. [12] made good progress; however, the models were very complex and hard to resolve.

The purpose of this study was to develop a practical model and an algorithm that could be used in the ESS allocation and operation process. In this study, a bi-level programming-based [13] model is presented, with the external and internal levels optimising allocation and operation, respectively. The model addresses both allocation and operation at the same time. Complexity assessment was used to simplify the model, which made this work a step forward towards the large-scale application of ESS. Another contribution of this work was to propose a genetic algorithm (GA)-based numerical algorithm to solve the mixed integer discrete non-linear model. Numerical experiments have the flexibility and applicability of the proposed model and algorithm.

2 Allocation and operation model

The bi-level programming problem (BLPP) is a hierarchical optimisation problem [14]. A distinguishing characteristic of the BLPP is that the decision variables at one level may affect the behaviour of a decision variable at another level [15]. The general BLPP is formulated as follows

$$\begin{aligned} &(\text{BLPP}) \min_x F(x, y) \\ &\text{s.t.} g(x, y) \le 0 \\ &\min_y f(x, y) \\ &\text{s.t. } h(x, y) \le 0 \end{aligned} \tag{1}$$

where $x \in R^{n_x}$ and $y \in R^{n_y}$ are decision variables of the external and internal levels, respectively. $F, f: R^{n_x}+n_y \to R$ are objective functions, and $g: R^{n_x}+n_y \to R^{n_u}$, $h: R^{n_x}+n_y \to R^{n_l}$ are constraints.

In the proposed model, objective functions and constraints are continuous and twice differentiable such that an optimal point exists theoretically.

2.1 External level

2.1.1 Objective function: The external level determines the ESS allocation, including the installation location, power rating, and energy rating. In general, there are two types of objectives related to the ESS allocation. One is to minimise the operation cost per day, which consists of the operation cost and power loss cost, when carrying out the demonstration projects to focus on the operation properties of the ESS. The other is to minimise the total cost per day, which consists of the ESS investment cost, operating cost, and power loss cost, when carrying out the real industrial projects. The two objective functions can be formulated as follows

$$\begin{aligned} &\min C_{\text{total}} = C_{\text{investment}} + C_{\text{generation}} + \eta_{\text{loss}} W_{\text{loss}} \\ &\text{or} \quad \min C_{\text{operation}} = C_{\text{generation}} + \eta_{\text{loss}} W_{\text{loss}} \end{aligned} \tag{2}$$

where $C_{\text{generation}}$ is the objective function of the internal level and is expressed in detail in Section 2.2.1. To choose C_{total} or $C_{\text{operation}}$ as the objective function of the external level depends on the purpose of the project. Generally, the investment cost is linearly correlated with the ESS power and energy rating [16], as shown below

$$C_{\text{investment}} = \sum_{k=1}^{N_s} \left(\frac{\eta_P P_{sk}^r + \eta_E E_{sk}^r}{T_{sk}} \right) \tag{3}$$

Power loss depends on the power flow results in every period, and is shown as

$$W_{\text{loss}} = \sum_t^T \Delta t \cdot \sum_i^N V_{i,t} \sum_{j \in i} V_{j,t} G_{ij} \cos \theta_{ij} \tag{4}$$

2.1.2 Constraints

(i) Power flow

$$\begin{cases} P_{\text{gi},t} + P_{\text{wi},t} + P_{si,t} - P_{\text{Li},t} = V_{i,t} \sum_{j \in i} V_{j,t} (G_{ij} \cos \theta_{ij,t} + B_{ij} \sin \theta_{ij,t}) \\ Q_{\text{gi},t} + Q_{\text{wi},t} + Q_{si,t} - Q_{\text{Li},t} = V_{i,t} \sum_{j \in i} V_{j,t} (G_{ij} \sin \theta_{ij,t} - B_{ij} \cos \theta_{ij,t}) \end{cases} \tag{5}$$

(ii) Voltage security

$$V_i^{\min} \le V_{i,t} \le V_i^{\max} \tag{6}$$

(iii) Transmission limit

$$0 \le P_{\text{l}ij,t} \le P_{\text{l}ij}^{\max} \tag{7}$$

(iv) Investment consideration

$$\begin{cases} 0 \le P_{sk}^r \le P_s^{\max} \\ 0 \le E_{sk}^r \le E_s^{\max} \end{cases}. \tag{8}$$

2.2 Internal level

2.2.1 Objective function: As indicated above, the external level determines the ESS allocation; the operation strategy is determined by the internal level. The ESS operation may not affect the unit commitment because the ESS control cycle is usually <1 h and the energy is limited. Thus, the internal level is a process of power dispatch rather than unit commitment, for both fossil-fuel generators and ESS. The internal objective function can be formulated as follows

$$\begin{aligned} \min C_{\text{generation}} = &\sum_{i=1}^{N_g} \sum_{t=1}^{T} (a_i P_{git}^2 + b_i P_{git} + c_i) \\ &+ \sum_{j=1}^{N_w} \sum_{t=1}^{T} \eta_w (P_{wjt}^{\max} - P_{wjt}) \cdot \Delta t + \sum_{k=1}^{N_s} \eta_{\text{Mk}} \end{aligned} \tag{9}$$

2.2.2 Constraints

(i) Power balance

$$\sum_{i=1}^{N_g} P_{\text{gi},t} + \sum_{j=1}^{N_w} P_{\text{w}j,t} + \sum_{k=1}^{N_s} P_{sk,t} - P_{\text{L},t} = 0 \tag{10}$$

(ii) Spinning reserve

$$\sum_{i=1}^{Ng} P_{\text{gi}}^{\max} + \sum_{j=1}^{Nw} P_{\text{w}j,t} + \sum_{k=1}^{Ns} P_{sk,t} - P_{\text{L},t} \ge R_t \tag{11}$$

(iii) Conventional generators generation constraint

$$P_{gi}^{\min} \le P_{gi,t} \le P_{gi}^{\max} \tag{12}$$

(iv) Conventional generators ramp limit

$$\left|P_{gi,t+1} - P_{gi,t}\right| \le r_{gi} \cdot \Delta t \tag{13}$$

(v) Wind farm generation constraint

$$0 \le P_{wj,t} \le P_{wj}^{\text{pre}} \tag{14}$$

(vi) ESS constraint

$$-P_{sk}^{\text{r}} \le P_{sk,t} \le P_{sk}^{\text{r}} \tag{15}$$

$$0 \le E_{sk,t} \le E_{sk}^{\text{r}} \tag{16}$$

$$E_{sk,t+1} = E_{sk,t} - \lambda_{sk} P_{sk,t} \cdot \Delta t \tag{17}$$

: A negative $P_{sk,t}$ value indicates that the ESS is charging while a positive value indicates discharging. In this study, it is assumed that energy storage efficiency is 1 such that the ESS maximum possible input/output power is equal to its power rating. P_{sk}^{r} and E_{sk}^{r} are obtained from the external level.

2.3 Effect of ESS type

Since no specific storage technology has been considered in the model, the methodology can be modified to consider any specific ESS type by changing several parameters.

The ESS type will affect the external objective function because different ESS types can have different technical parameters such that the investment cost, operation cost, and power loss vary in different degrees. As for the internal level, the duration of each period Δt is the key parameter. In terms of its function, the ESS type can be categorised into power ESS and energy ESS. Power ESS shows good characteristics for pulse power but cannot provide stable and continuous power output so that Δt cannot be set too long. However, if Δt is too short, then the computation time is too long so that the algorithm cannot be applied in real-world applications. The selection of Δt is a trade-off between validity and computation speed. In this work, Δt of power ESS is set to 15 min and that of energy ESS is 1 h.

3 Model simplification

After complexity assessment, it was found that the external level is a mixed integer discrete non-linear programming and the internal level is a large-scale quadratic programming.

The external level complexity can be divided into two parts; ESS allocation optimisation results in the mixed integer discrete complexity, which is related to the number of ESSs, and power flow computation results in the non-linear complexity, which is related to the scale of power system. The external level is not easy to simplify because the number of ESSs or scale of the power system is determined by demand and cannot be modified.

The internal objective function is quadratic and the constraints are linear. The number of variables in the internal level can be expressed as follows

$$\frac{24}{\Delta t}(N_{\text{g}} + N_{\text{w}} + 2N_{\text{s}}) \tag{18}$$

If there are nine fossil-fuel generators, one wind farm, two ESSs, and Δt equals to 15 min, then the number of variables can reach 2208. Mathematically, this approach is called large-scale quadratic programming, and computation is time consuming. To solve this problem, as shown in Fig. 1, the quadratic fossil-fuel generator cost in (9) can be accurately approximated by a set of piecewise segments [17, 18] to make the internal level a linear programming.

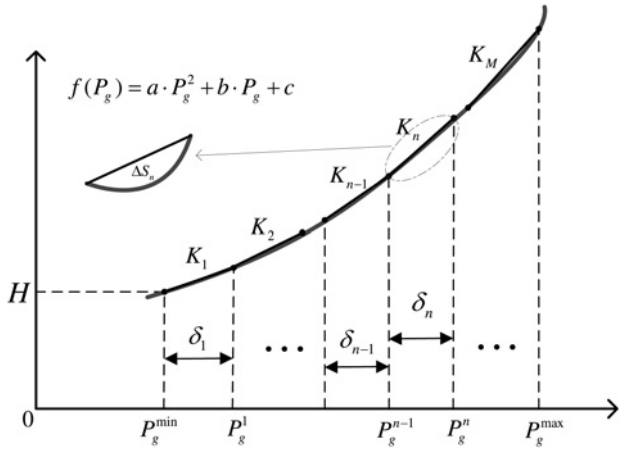

Fig. 1 *Piecewise linear generation cost*

Assume that the number of segments is M and the slope of the nth segment is given the following equation

$$\begin{aligned} K_n &= \frac{f(P_{\text{g}}^n) - f(P_{\text{g}}^{n-1})}{P_{\text{g}}^n - P_{\text{g}}^{n-1}} \\ &= \frac{[a(P_{\text{g}}^{n-1} + \delta_n)^2 + b(P_{\text{g}}^{n-1} + \delta_n) + c] - [a(P_{\text{g}}^{n-1})^2 + bP_{\text{g}}^{n-1} + c]}{\delta_n} \\ &= a\delta_n + 2aP_{\text{g}}^{n-1} + b \end{aligned} \tag{19}$$

The deviation between the piecewise segment and quadratic curve can be expressed as the area of ΔS, as shown in Fig. 1. Note that every point from the segments is above the quadratic curve; this is because the coefficient a is positive. The nth deviation is expressed as follows

$$\begin{aligned} \Delta S_n &= \int_0^{\delta_n} [f(P_{\text{g}}^{n-1}) + K_n x - f(P_{\text{g}}^{n-1} + x)]\text{d}x \\ &= \int_0^{\delta_n} [a(P_{\text{g}}^{n-1})^2 + bP_{\text{g}}^{n-1} + c + K_n x]\text{d}x \\ &\quad - \int_0^{\delta_n} [a(P_{\text{g}}^{n-1} + x)^2 + b(P_{\text{g}}^{n-1} + x) + c]\text{d}x \\ &= \frac{1}{6} a \delta_n^3 \end{aligned} \tag{20}$$

Such that the total deviation is

$$\begin{aligned} \Delta S &= \sum_n \Delta S_n = \frac{1}{6} a \sum_{n=1}^{M} \delta_n^3 \ge \frac{1}{6} a \cdot M \cdot \left(\frac{\sum \delta_n}{M}\right)^3 \\ &= \frac{a(P_{\max} - P_{\min})^3}{6M^2} \propto \frac{1}{M^2} \end{aligned} \tag{21}$$

If and only if

$$\delta_1 = \delta_2 = \cdots = \delta_M = \frac{P_{\text{g}}^{\max} - P_{\text{g}}^{\min}}{M} \tag{22}$$

Table 1 shows that the computation time increases and the relative error decreases as the total number of segments increases. In this work, M is equal to 3 for both practical and theoretical considerations. The analytic representation of this linear

Table 1 Computation time and the relative error of the total number of segments

Number of segments	Computation time, s	Relative error rate, 1/M^2
1	0.2487	1.0000
2	0.2583	0.2500
3	0.2615	0.1111
4	0.2682	0.0625
5	0.2741	0.0400

approximation is

$$\begin{cases} P = P_{\mathrm{g}}^{\min} + p_1 + p_2 + p_3 \\ f \simeq a \cdot (P_{\mathrm{g}}^{\min})^2 + b \cdot P_{\mathrm{g}}^{\min} + c + K_1 p_1 + K_2 p_2 + K_3 p_3 \end{cases} \tag{23}$$

where p_1, p_2, p_3 are new variables in the linear programming to replace P_{g} in the quadratic programming, which is determined by

$$\begin{cases} 0 \le p_1 \le \delta_1, \quad p_2 = 0, \ p_3 = 0 \\ 0 < p_2 \le \delta_2, \quad p_1 = \delta_1, \ p_3 = 0 \\ 0 < p_3 \le \delta_3, \quad p_1 = \delta_1, \ p_2 = \delta_2 \end{cases} \tag{24}$$

δ_i and K_i can be calculated from (19) and (22)

$$\begin{cases} \delta_1 = \delta_2 = \delta_3 = \dfrac{P_{\mathrm{g}}^{\max} - P_{\mathrm{g}}^{\min}}{3} \\ K_1 = a\left(\dfrac{1}{3}P_{\mathrm{g}}^{\max} + \dfrac{5}{3}P_{\mathrm{g}}^{\min}\right) + b \\ K_2 = a(P_{\mathrm{g}}^{\max} + P_{\mathrm{g}}^{\min}) + b \\ K_3 = a\left(\dfrac{5}{3}P_{\mathrm{g}}^{\max} + \dfrac{1}{3}P_{\mathrm{g}}^{\min}\right) + b \end{cases} \tag{25}$$

The number of variables in the simplified internal level is

$$\frac{24}{\Delta t}(3N_{\mathrm{g}} + N_{\mathrm{w}} + 2N_{\mathrm{s}}) \tag{26}$$

Although the dimension increases from (18) to (26), the linear programming is solved more easily and quickly than the quadratic programming.

4 Numerical algorithm

Since the model has a great computation complexity [18] and cannot be easily solved using conventional optimisation tools, a GA-based numerical algorithm is proposed.

Fig. 2 shows the flowchart of the numerical algorithm. The power system parameters and day-ahead wind power output and load forecasts are inputs to the model. Since the internal level has been simplified to a linear programming, it is optimised by the classical interior point algorithm, which is shown as 'internal optimisation' in Fig. 2. In step 1, an initial generation consisting of 30 chromosomes is randomly generated. The chromosome represents the binary code string of decision variables in the external level; the installation location is encoded by the grey code, while the power and energy rating are encoded by the binary code. As the newly generated chromosome may exceed constraints, the feasibility test is necessary. The feasibility test (step 2) mainly judges the solvability of the internal optimisation and power flow computation. The unfeasible chromosome is rejected and another one is randomly regenerated until the initial generation is feasible and full. In step 3, the fitness function of each chromosome is calculated according to (2). In step 4, offspring generation is generated through nature evolution, which is simulated by selection, crossover, and mutation. Note that both crossover and mutation generate new chromosomes, and the feasibility test is also necessary. The block 'feasibility test' in step 4 contains the same steps in step 2. Repeat steps 3 and 4 until the number of generations is equal to 100.

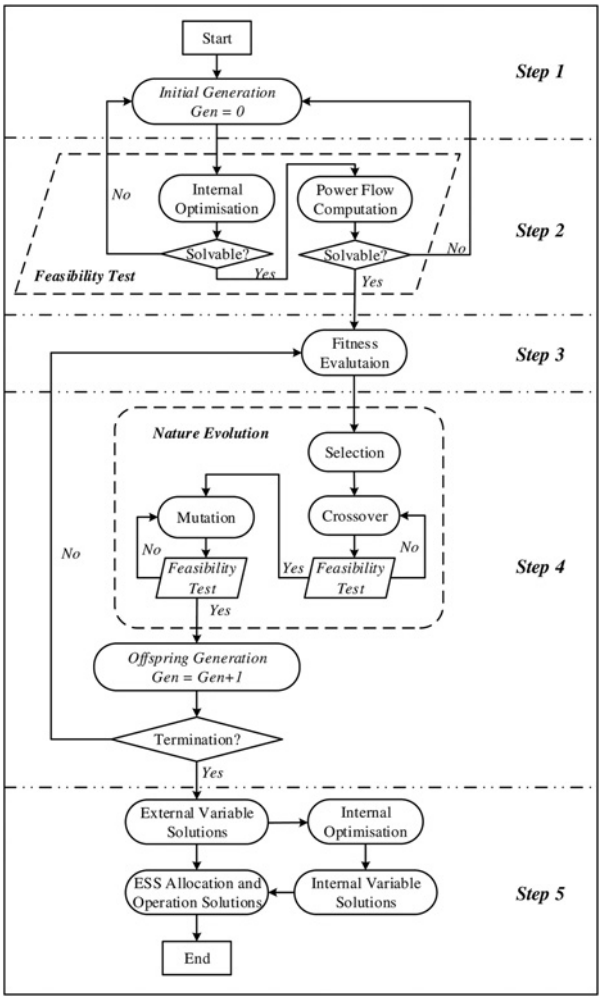

Fig. 2 *Algorithm flowchart*

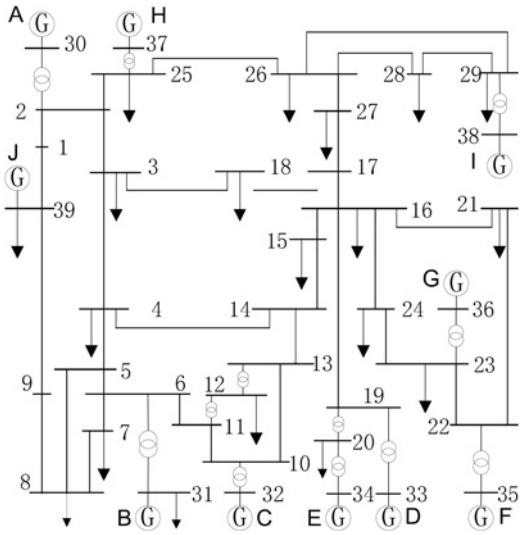

Fig. 3 *IEEE 39 bus system*

Table 2 Introduction of cases based on the IEEE 39 bus system

Case	ESS type	E_s^{min}, p.u.	E_s^{max}, p.u.	P_s^{min}, p.u.	P_s^{max}, p.u.	Number of ESSs	Optimal target
1	PHS	24	24	0.5	4	1	minimum total cost
2	PHS	24	24	0.5	4	1	minimum operation cost
3	FBS	0.5	5	0.05	0.5	2	minimum total cost
4	FBS	0.5	5	0.05	0.5	2	minimum operation cost

5 Numerical experiments and analysis

To illustrate the flexibility of the model and the applicability of the numerical algorithm, it has been applied in two example systems. All of the numerical experiments were performed on a PC with an Intel i5 CPU 3.19-GHz clock and 2 GB RAM.

5.1 Flexibility

The first example system is a modified IEEE 39 bus system, as shown in Fig. 3. In the modified system, generator F is replaced with real data from a wind farm in Inner-Mongolia, China. Four cases were designed to test the flexibility of the model. The parameters of the cases varied in ESS types and optimal targets, as shown in Table 2. The energy rating of pumped hydroelectric storage (PHS) is determined by geographical conditions such that E_s^{max} is equal to E_s^{min} in cases 1 and 2. The transmission limit from bus 35 to bus 22 is 450 MW. The wind farm's day ahead predictive and actual power output without ESS is shown in Fig. 4. As shown in Fig. 4, wind curtailment occurs mainly due to two reasons. One is because wind is large in off-peak hours and the system cannot absorb excess energy, such that the curtailment occurs from 3:00 to 6:00. The other is because the wind farm power rating is greater than the transmission limit such that excess energy cannot be delivered to load the centre in a timely manner, which is also known as congestion, such that the curtailment occurs from 22:00 to 24:00. The physical system is normalised into units, with the power base value equals to 100 MVA.

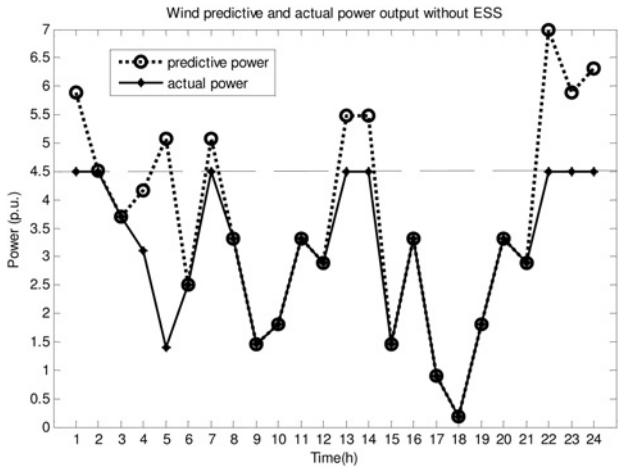

Fig. 4 *Wind predictive and actual power output in congestion scenario*

The numerical experiment results are assembled in Table 3. It is observed that the total cost increases dramatically while the operation cost decreases slightly as the ESS power and energy rating increase. This is because the ESS investment cost is much more than the loss caused by wind curtailment at the present stage. Thus, the solutions of power and energy rating in cases 1 and 3 reach a minimum; the wind curtailment reduction is less than that of cases 2 and 3, respectively. Specific wind curtailment is necessary in real operations to decrease the total cost. When compared cases 1 and 3, or cases 2 and 4, it is obvious that PHS is more appropriate than flow battery storage (FBS) because PHS is cheaper than FBS and has a greater power and energy capacity to address the integration of wind power.

When analysing the installation location shown in Table 3, it is interesting to find that ESS tends to be installed at buses 30 and 35. We carried out more case studies on the IEEE 39 bus system, as shown in Table 4. It illustrates that ESS being installed at buses 30 and 35 is not computed by chance.

To explain the results, we should look back to analyse the objective functions of our optimisation. As indicated in (9), the object of the internal level is to minimise the generation cost. The generation cost consists of three parts: conventional generation costs, wind curtailment penalty, and ESS operation cost, which is considered constant. Reducing wind curtailment will increase wind power generation and further decrease conventional generation cost. Thus, minimising generation cost equals to reducing wind curtailment. Note that bus 35 is the point of common coupling) bus near the wind farm. ESS installed at bus 35 can reschedule the power flow of the transmission line 35–22 and absorb the excess wind energy that may be curtailed due to congestion. This is the reason why ESS tends to be installed at bus 35.

On the other hand, as shown in (2), the object of the external level is to minimise the operation cost or the total cost, both of which comprise the power loss fraction. It should be noted that ESS installation location will affect the power loss of the system by

Table 3 Results of case studies based on the IEEE 39 bus system

Case	Installation location	Power rating, p.u.	Energy rating, p.u.	Wind curtailment reduction, p.u.	Operation cost, $	Total cost, $
1	bus 35	0.50	24	4.52	137,470	204,593
2	bus 35	3.82	24	14.37	133,420	427,940
3	bus 30/35	0.05/0.05	0.50/0.50	0.21	139,250	327,606
4	bus 30/35	0.49/0.5	1.79/4.16	5.52	137,060	1,460,690

Table 4 Introduction and installation location results of supplementary case studies based on the IEEE 39 bus system

Case	ESS type	Number of ESSs	Optimal target	Installation location	Power rating, p.u.	Energy rating, p.u.
7	PHS	2	minimum total cost	bus 30/35	0.50/0.5	24/24
8	PHS	2	minimum operation cost	bus 30/35	3.61/3.82	24/24
9	FBS	3	minimum total cost	bus 30/34/35	0.05/0.05/0.05	0.50/0.50/0.50
10	FBS	3	minimum operation cost	bus 30/35/37	0.50/0.50/0.48	3.71/3.80/4.33

Table 5 Power loss sensitivities

Bus	Sensitivity	Bus	Sensitivity	Bus	Sensitivity
3	0.2250	4	0.2230	7	0.1939
8	0.2304	12	0.1026	15	0.1981
16	0.1682	18	0.2197	20	0.1310
21	0.1360	23	0.0812	24	0.1608
25	0.1248	26	0.1508	27	0.1933
28	0.1334	29	0.0911	30	−0.1550
31	0.0046	32	0.2554	33	−0.0164
34	−0.0598	35	0	36	−0.0119
37	−0.0502	38	0.0138	39	0.2234

changing the reactive power flow in the grid. Table 5 shows the power loss sensitivity of other generation and load buses to the wind farm bus (i.e. bus 35). It is determined that the sensitivity of bus 30 to bus 35 is minimal among all generation and load buses. Thus, the ESS installed at bus 30 can reduce power loss effectively. This can also explain why the FBS is installed at bus 34 or bus 37 in the supplementary case studies.

5.2 Applicability

The other example system is a provincial regional power system in central China, as shown in Fig. 5. It contains 83 fossil-fuel generators, 8 wind farms, and 1006 buses. Two ESSs are allocated in the system. The raw data pre-processing method can be found in [19]. The real system is used to test the applicability of the numerical algorithm, that is the computation time and convergence when dealing with a large-scale system. Cases 5 and 6 are designed based on the system. There are two sets of FBS applied in the provincial regional power system. The FBS's maximum power rating is 5 MW and energy rating is 10 MWh. The charge/discharge efficiency is 70% and the total investment cost is around 10 million US dollars. To compare the computation speed and convergence speed between the modified IEEE 39 bus system and the provincial regional power system, the computation time and convergence generation of both systems are recorded, as shown in Table 6.

According to the algorithm flowchart, the power flow and internal optimisation computation are basic components of the algorithm. Power flow time and internal optimisation time are the average time of power flow and internal optimisation computation, respectively. The power flow time is related to the number of system buses while the internal optimisation time is related to the dimension of internal optimisation. The power flow time remains nearly constant from case 1 to case 4 and from case 5 to case 6. However, as the duration of each period Δt decreases from 1 h to 15 min, the dimension of the internal optimisation is three times larger in cases 3 and 4 than that in cases 1 and 2. The internal optimisation time increases as the dimension of internal optimisation increases.

Convergence generation is defined as the first generation that the following generations' best fitness remains constant. It is observed that the algorithm converged at no more than 60 generations. According to many literatures that consider the effects of GA parameters to its convergence speed, the best results occurred for a smaller population size combined with a relatively high mutation rate. Thus, the population size is set to 30 and the mutation rate is set to 0.20 after several parameter sweep experiments in this work.

Table 6 shows that the algorithm has both good computation and convergence characteristics; thus, the model can be applied in a large-scale system.

From the case studies above, several conclusions are summarised as follows:

(i) the investment cost of ESS is high such that some wind curtailment is necessary to minimise total cost and to stabilise the power system;
(ii) PHS has a proper power rating and energy rating to make it an ideal type of large-scale ESS in the integration of wind;
(iii) FBS is far from large-scale applicable due to limited energy rating and high price;

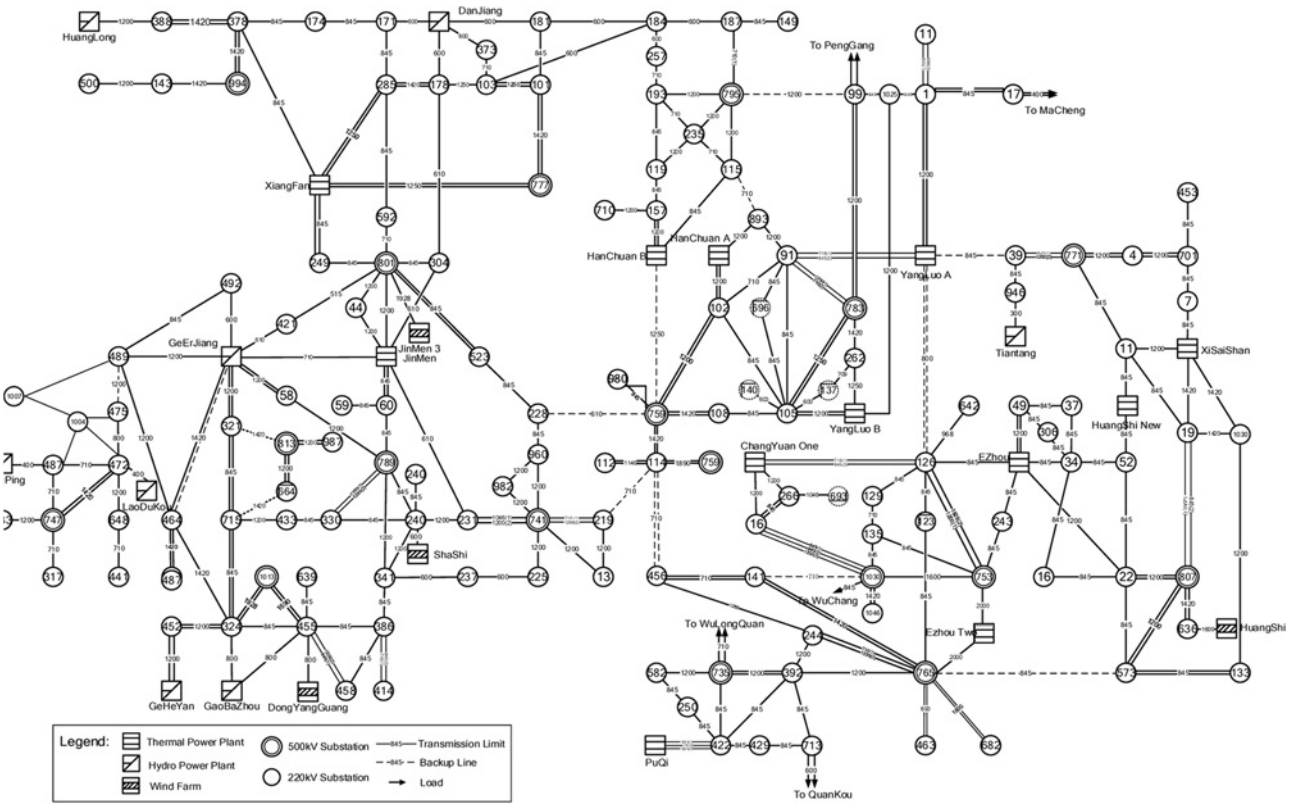

Fig. 5 *Provincial regional power system*

Table 6 Computation time of case studies

Case	Total computation time, s	Power flow time, s	Number of system buses	Internal optimisation time, s	Dimension of internal optimisation	Convergence generation
1	282.09	0.0108	39	0.0349	720	37
2	281.90	0.0108	39	0.0346	720	34
3	1062.4	0.0101	39	0.1990	3072	37
4	1095.2	0.0104	39	0.2016	3072	26
5	2085.3	0.0665	1006	0.6165	6264	56
6	2107.1	0.0687	1006	0.6093	6264	49

(iv) without accurate simulation and computation, ESS tends to be installed in two types of buses. One is the bus near the transmission congestion line to decrease congestion-induced curtailment. The other is the bus with a minimum power loss sensitivity relative to the wind farm bus to optimise the reactive power flow and to reduce power loss.

6 Conclusions

In this paper, the contribution of the ESS to the operation of a large-scale power system with high wind penetration has been studied with the help of an optimal allocation and operation model based on bi-level programming. The effectiveness of the proposed method and algorithm has been tested with comprehensive case studies, that is an IEEE standard test system and a regional power system in China. The system operation has also been studied under different demand and wind speed scenarios.

The methodology presented in this paper could serve as a basis for economic feasibility studies of ESS facilities, and even to help decision makers in the energy sector have better insight with a more reasonable ESS allocation and operation blueprint integrating wind energy.

7 Acknowledgments

This work was supported by National High Technology Research and Development Program of China (863 Program) (2012AA050207), Science and Technology Projects of the State Grid Corporation of China (SGZJ0000BGJS1300438), Science and Technology Projects of Hunan Electric Power Company (SGHN0000DKJS1300221), and Science and Technology Projects of Ningxia Electric Power Company (SGNX0000DKJS1400685).

8 References

1 Chinese Wind Energy Association (CWEA): 'Chinese wind power capacity assessment in 2013', *Wind Energy Ind.*, 2013, **3**, pp. 14–18

2 Wu, J.: 'Research on technology problems of large grid-connected wind farm'. PhD thesis, Tsinghua University, 2004

3 Atwa, Y.M., El-Saadany, E.F.: 'Optimal allocation of ESS in distribution systems with a high penetration of wind energy', *IEEE Trans. Power Syst.*, 2010, **25**, (4), pp. 1815–1822

4 Mohammadi, S., Mozafari, B., Solymani, S., *et al.*: 'Stochastic scenario-based model and investigating size of energy storages for PEM-fuel cell unit commitment of micro-grid considering profitable strategies', *IET Gener. Transm. Distrib.*, 2014, **8**, (7), pp. 1228–1243

5 Ross, M., Hidalgo, R., Abbey, C., *et al.*: 'Energy storage system scheduling for an isolated microgrid', *IET Renew. Power Gener.*, 2011, **5**, (2), pp. 117–123

6 Yuan, Y., Li, Q., Wang, W.: 'Optimal operation strategy of energy storage unit in wind power integration based on stochastic programming', *IET Renew. Power Gener.*, 2011, **5**, (2), pp. 194–201

7 Daneshi, H., Srivastava, A.K.: 'Security-constrained unit commitment with wind generation and compressed air energy storage', *IET Gener. Transm. Distrib.*, 2012, **6**, (2), pp. 167–175

8 Brekken, T.K.A., Yokochi, A., von Jouanne, A., *et al.*: 'Optimal energy storage sizing and control for wind power applications', *IEEE Trans. Sustain. Energy*, 2011, **2**, (1), pp. 69–77

9 Teleke, S., Baran, M.E., Bhattacharya, S., *et al.*: 'Optimal control of battery energy storage for wind farm dispatching', *IEEE Trans. Energy Convers.*, 2010, **25**, (3), pp. 787–794

10 Chen, C., Duan, S.: 'Optimal allocation of distributed generation and energy storage systems in microgrids', *IET Renew. Power Gener.*, 2014, **8**, (8), pp. 581–589

11 Zheng, Y., Dong, Z.Y., Luo, F.J., *et al.*: 'Optimal allocation of energy storage system for risk mitigation of DISCOs with high renewable penetrations', *IEEE Trans. Power Syst.*, 2013, **99**, pp. 1–9

12 Chakraborty, S., Senjyu, T., Toyama, H., *et al.*: 'Determination methodology for optimizing the energy storage size for power system', *IET Gener. Transm. Distrib.*, 2009, **3**, (11), pp. 987–999

13 Liu, H.: 'Study on the theory and algorithms of multilevel programming problem'. PhD thesis, Xidian University, 2000

14 Dempe, S.: 'Annotated bibliography on bilevel programming and mathematical programs with equilibrium constraints', *Optimization*, 2003, **52**, pp. 333–359

15 Wang, G., Wan, Z., Wang, X.: 'Bibliography on bilevel programming', *Adv. Math.*, 2007, **36**, (5), pp. 513–529

16 Chen, H., Cong, T.N., Yang, W., *et al.*: 'Progress in electrical energy storage system: a critical review', *Prog. Nat. Sci.*, 2009, **19**, (3), pp. 291–312

17 Carrion, M., Arroyo, J.M.: 'A computationally efficient mixed-integer linear formulation for the thermal unit commitment problem', *IEEE Trans. Power Syst.*, 2006, **21**, (3), pp. 1371–1378

18 Zhang, F., Hu, Z., Song, Y.: 'Mixed-integer linear model for transmission expansion planning with line losses and energy storage systems', *IET Gener. Transm. Distrib.*, 2013, **7**, (8), pp. 919–928

19 Zheng, L., Hu, W., Min, Y.: 'Raw wind data preprocessing: a data-mining approach', *IEEE Trans. Sustain. Energy*, 2015, **6**, (1), pp. 11–19